PERGAMON

Carbon 38 (2000) 831–838

CARBON

Characterization of interfaces in C fiber-reinforced laminated C–SiC matrix composites

K.A. Appiah[a], Z.L. Wang[a,*], W.J. Lackey[b]

[a]*School of Materials Science and Engineering, Georgia Institute of Technology, Atlanta, GA 30332, USA*
[b]*School of Mechanical Engineering, Georgia Institute of Technology, Atlanta, GA 30332, USA*

Received 12 March 1999; accepted 30 July 1999

Abstract

Interfacial studies of carbon fiber-reinforced laminated matrix composites (LMCs) of alternating matrix layers of SiC and carbon prepared by forced-flow thermal-gradient chemical vapor infiltration (FCVI) have been undertaken by transmission electron microscopy (TEM). The carbon–carbon interfacial region consistently displayed distinctive features that enabled the microstructures of the fiber carbon, a thin carbon layer deposited as fiber coating, and the matrix carbon to be distinguished. A thin discontinuous layer of relatively lower graphitic degree was observed at the interface of the fiber and its carbon coating, whereas the interface between the fiber coating and the first carbon layer of the matrix displayed a thin, patchy, and partially ordered layer. At the C–SiC interfaces within the matrix, the interface was observed to be well-defined on one side with the *c*-axis of the pyrocarbon layers nearly perpendicular to the interface, but, at the other end, the interface appeared rough and somewhat diffuse due to the nature of SiC growth during CVI.

Keywords: A. Carbon composites; B. Chemical vapor infiltration (CVI); C. Transmission electron microscopy (TEM); D. Microstructure

1. Introduction

Composites possessing properties such as high-temperature strength retention, high toughness, creep resistance, and low density which are desirable for structural applications have been quite extensively investigated. The composite systems that have been studied include whisker-reinforced glasses [1], whisker-reinforced ceramics [2–5], and, more notably, SiC fiber-reinforced ceramic matrices [6–9]. The choice of fiber coating and matrix-reinforcement pairs is largely dictated by chemical compatibility, similar thermal expansivities due to the anticipated high-temperature applications of these materials, and ease of fabrication [10].

In these composite systems, microstructural characterization of the fiber–matrix interface provides some insight into the mechanical behavior of the composites. The fiber–matrix interface is desired to be strong enough to allow load transfer from the matrix to the fiber while remaining sufficiently weak to allow the fiber to easily debond to arrest crack propagation, thereby improving toughness. In most SiC fiber-reinforced composites, a carbon-rich interfacial layer deposited as fiber coating or formed due to an interfacial reaction is known to enhance the fracture toughness of the material, although oxidative instability at high temperatures then becomes a concern [6–11]. Also, the nature and extent of fiber surface roughness has been found to contribute to improved toughness [12–14], but, generally, an optimum interfacial coating thickness is believed to be more beneficial to toughness improvements by enabling debonding within the coating [10].

Laminated matrix composite materials (LMCs) promise toughness improvements by combining the benefits of lamination with those of traditional fiber reinforcements [15]. The multiple layers of the laminated matrix have the potential to arrest crack propagation by enabling crack deflection and branching. In fact, deliberate fracture of these composites have shown the crack paths to be tortuous within the laminated matrix [15]. Also, the anisotropic and layered structure of carbon should allow for easy debonding at fiber–matrix interfaces. Furthermore, the SiC layers could form the oxide to protect the carbon from high-temperature oxidation [16,17].

Since laminated matrix composites are a relatively new

*Corresponding author. Tel.: +1-404-894-8008; fax: +1-404-894-9140.

E-mail address: zhong.wang@mse.gatech.edu (Z.L. Wang).

0008-6223/00/$ – see front matter
PII: S0008-6223(99)00177-3

class of promising materials, it is essential that an analysis and understanding of the interfacial microstructure, critical to the mechanical behavior of the material, be acquired to help the fabrication effort in obtaining composites that will exhibit the desired mechanical behavior. Thus, the focus of this study was to obtain detailed information on the interfacial microstructure of these laminated composites to enable subsequent improvements in the processing.

Electron microscopy techniques are well suited to the characterization of the microstructure of these composites. In particular, transmission electron microscopy can provide detailed structural information on the interfacial microstructure at a high image resolution. There is a scarcity of published work on such detailed TEM investigations of interfacial microstructures. In this work, we present the results of detailed microstructural characterization of the carbon–carbon interfacial zones between the matrix and fiber and the SiC–C interfaces between the matrix layers.

2. Experimental procedure

2.1. Composite manufacture

The SiC–C LMCs were fabricated by forced-flow thermal-gradient chemical vapor infiltration (FCVI) of T-300 grade fibrous carbon preforms. The preforms consisted of 40 layers of plain weave cloth stacked in a graphite holder at 0–90°. Details of the FCVI fabrication process, parameters, and reactor configuration for this composite have been previously described by Lackey et al. [15]. Briefly, during the FCVI process, the reagent gases are forced to flow through the fibrous carbon preforms. The reagent streams are altered to deposit the different matrix components alternately. The carbon of the fiber coating was deposited from a mixture of methane and hydrogen while the carbon layers of the matrix were deposited from a mixture of propylene–hydrogen. The SiC layers were deposited from a mixture of methyltrichlorosilane (MTS) and hydrogen.

2.2. TEM sample preparation

Specimens for TEM examination were obtained by cutting ~1 mm thickness (cross-sectional with respect to fiber axes) slices with a low-speed diamond wafering saw (Buehler) from a bulk sample which had been previously embedded in epoxy resin. The slices were then mounted again in epoxy, polished, dimpled to a center thickness of ~30 μm, and, subsequently, ion-milled to electron transparency. The ion milling (E.A. Fischione Instruments) was performed with argon at cryogenic temperatures (liquid N_2) on a rotating stage and at a voltage of 4 kV. The milling angle was gradually lowered from the initial 15° to 5° as milling progressed. TEM imaging was performed using a JEOL 4000EX high-resolution microscope operating at 400 kV with a point-to-point image resolution of 0.18 nm. Both the bright-field and dark-field images were recorded using an objective aperture of radius 4 mrad. High-resolution TEM images were recorded using an objective aperture that is large enough to enclose the {004} reflection of graphite. Scanning electron microscopy (SEM) work was done using a HITACHI FEG S800 SEM.

3. Results and discussion

3.1. Fiber-matrix (C–C) interfaces

In Fig. 1, the SEM image shows the cross-sectional view of the general morphology of the composite with individual fibers (circular disks) surrounded by the matrix. The matrix materials fill up the spaces between the fibers leaving some level of porosity that is usually typical in the CVI process. Fig. 2 shows a bright-field TEM cross-sectional image of the composite material. The matrix is clearly seen to consist of layers of alternate carbon (light) and SiC (dark) layers with progression from the fiber surface. The layers are seen to increase in thickness with distance from the fiber surface. At this magnification, the deposited carbon interfacial coating cannot be easily distinguished from the first carbon layer of the matrix. In

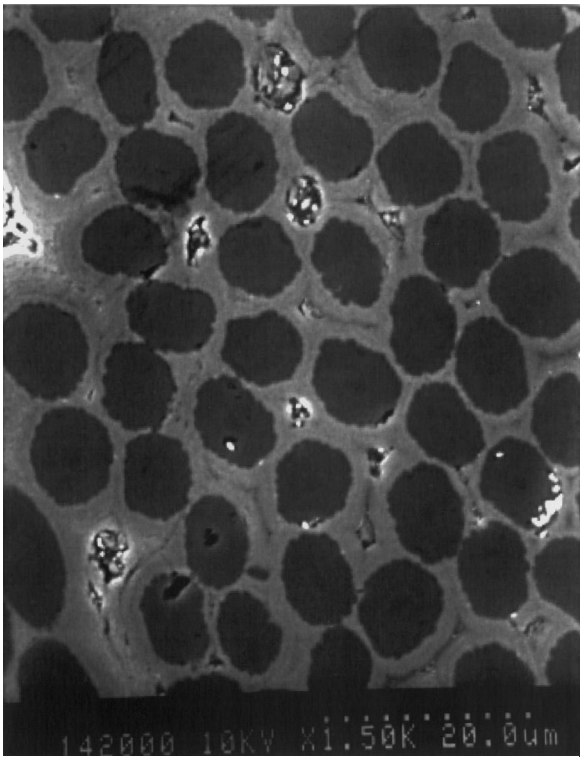

Fig. 1. An SEM image showing the general morphology of the composite.

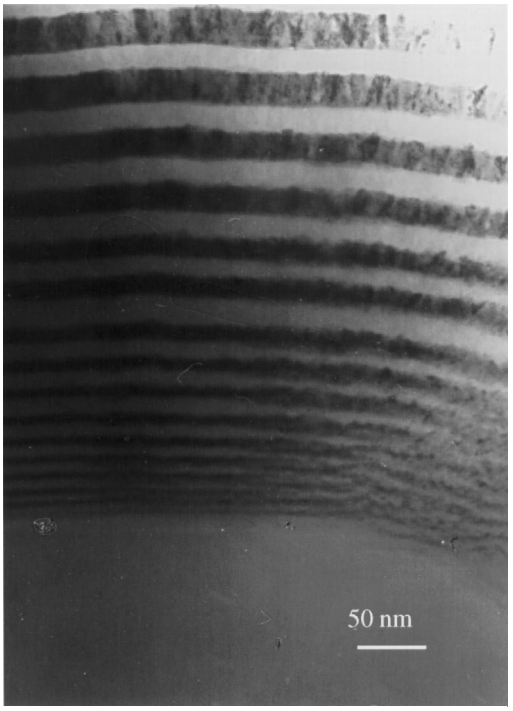

Fig. 2. A bright-field TEM cross-sectional image of the composite showing the progression of matrix layers from fiber surface.

Fig. 3a and b, bright-field and corresponding dark-field images, respectively, of the matrix layers are shown. To reveal the grain size of SiC, the dark-field image was recorded by an objective aperture of 4 mrad in radius using the {111} and {200} reflections. The growth and development of the SiC layers are evident in these micrographs. The dark-field image of Fig. 3b shows that the sizes of the SiC crystals are approximately of the order of the layer thickness, and thus the SiC layer thickness is controlled by the crystal growth. The diffraction pattern inset shows that there appears to be a parallel orientation relationship between the pyrocarbon and β-SiC layers.

Fig. 4 captures, in sequence, a view of the carbon fiber, the carbon fiber coating, and the first two matrix layers of carbon and silicon carbide with intervening interfacial features. Beginning from the top of the micrograph, the graphite layers of the fiber appear to be only partially ordered in comparison to the seemingly higher graphitic degree (i.e. higher basal plane alignment) exhibited by the subsequent carbon of the fiber coating. A close look at the high-resolution cross-sectional image of the carbon fiber in Fig. 5 allows for the microstructure to be distinguished from that of the coating and the matrix. The fiber coating and matrix carbons are seen to possess wavy features typical of TEM images of smooth laminar carbons [18,19] and exhibit some amount of preferred orientation, whereas the fringes of the fiber carbon present as relatively more randomly oriented arcs. Indeed, it may be argued that the graphitic basal planes of the coating appear to be slightly more aligned than that of the first carbon layer of the matrix.

As indicated in Fig. 4, a thin and somewhat discontinuous layer (that may not be readily apparent) is observed at the interface of the fiber and its coating. In Fig. 6, this transitional layer which is seen to be clearly less-ordered and lies at the interface of the fiber and the fiber coating is indicated (by arrows). Another patchy and fragmented layer of a partially crystalline material is seen in the TEM image, lying in the middle of the fiber coating–matrix carbon band. This layer is expectedly at the interface of the fiber coating and the first carbon layer of the matrix as evidenced by the thickness (~10 nm as expected of the first carbon layer of the matrix) of the pyrocarbon layer below it.

Typically, carbon exhibits varied microstructures depending on processing variables such as temperature, pressure, and flow rates employed during processing, and the type and nature of reagent gases and intermediate species formed during the pyrolytic deposition. It is well known that, in general, it is difficult to predict a priori the microstructure of carbon from the processing conditions employed, since most of the processing–microstructure relationships have been derived empirically [20,21] and are not clearly understood. Although research work by Lieberman and Pierson [22,23], and, more recently, Lewis et al. [24] have advanced models to explain how the microstructure of CVI pyrolytic carbon depends on the infiltration conditions, the microstructure has usually been discussed at the lower spatial resolution levels of optical microscopy and SEM. Thus, there is a real need to obtain high-spatial resolution microstructural information on pyrolytic carbon to which processing conditions can be correlated.

Based on the dearth of published information that correlates the high resolution (TEM) microstructure of pyrolytic carbon to the processing conditions employed and other factors, the microstructural features on the carbon–carbon interfaces presented in this work may not be easily explained. However, it must be noted that the published work by other researchers have shown the existence of a thin transitional layer at the fiber-coating interface that is believed to be induced by the roughness of the fiber surface [18,19]. The extent and thickness of this transitional layer is believed to increase with an increase in the degree of graphitic order of the fiber, and hence, its type. In agreement with other reported results [18], the transitional layer at the fiber-coating interface in Fig. 6 is observed to be very thin and disordered (~8 nm) due to the previously mentioned rough surface and lower graphitic degree of the fiber (T-300 grade) used in this work. Also, the fiber-coating interface would not be expected to be very obvious because, in general, amorphous-crystalline phase boundaries do not create any marked contrast effects

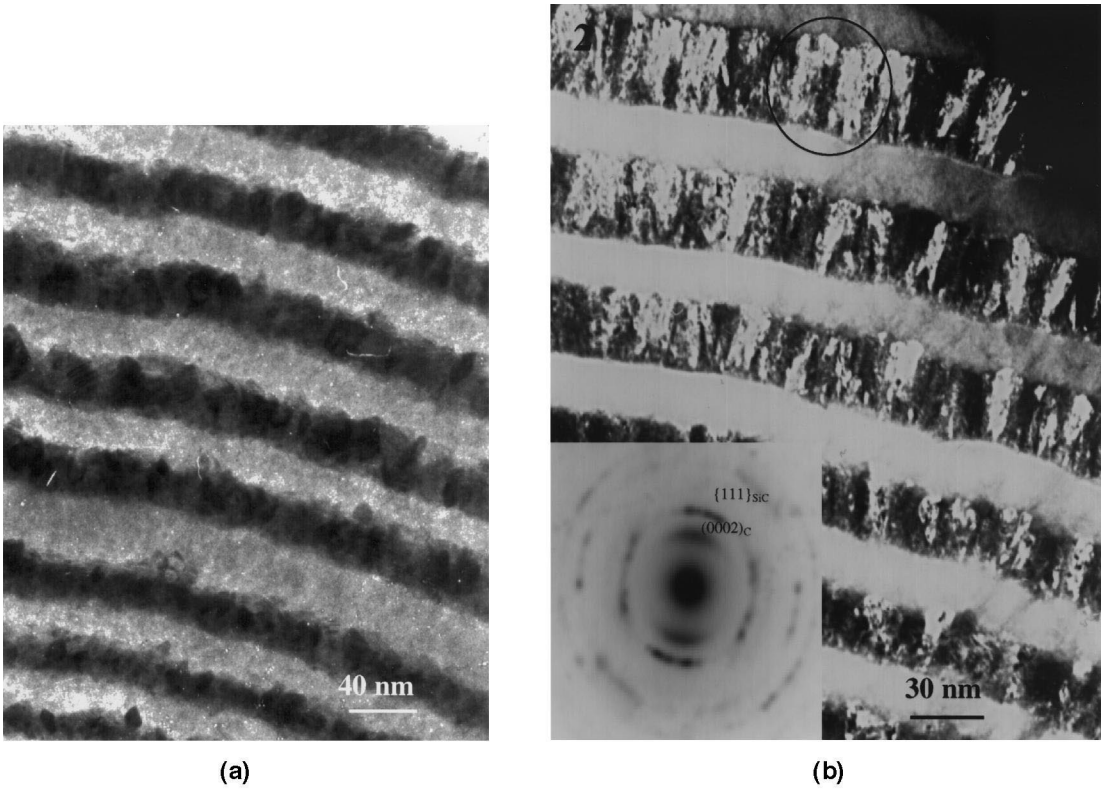

Fig. 3. (a) A bright-field TEM image showing the morphology of the matrix layers. (b) A dark-field TEM image showing SiC crystals. Diffraction pattern (inset) reveals parallel orientation relationship between C and SiC matrix layers.

in bright-field TEM imaging. In addition, there is no compositional contrast between the two layers.

At the C–C interface of the fiber coating and the first matrix carbon layer, the reasons for the occurrence of the patchy and partly ordered layer is not understood. It is highly likely that the switch from methane to propylene as the reagents used to deposit the coating and matrix carbons, respectively, possibly engenders the formation of a partially ordered phase. During CVI/CVD of pyrocarbon, ordered and more crystalline phases such as diamond-like carbons, which are metastable to the formation of graphite, may form in the presence of an activated species and/or atomic hydrogen which etches the graphite away. Although, hydrogen gas was made to flow through the preform between depositing the coating and the matrix carbon, the mechanism by which atomic hydrogen may have been possibly induced remains to be investigated.

The microstructures of the coating and matrix carbons are hard to differentiate because both methane [20] and propylene [18] are known to yield laminar carbon structures during CVI, as observed in this work. Additionally, propylene is believed to be a possible intermediate product during pyrocarbon deposition from methane and vice-versa [25].

3.2. SiC–carbon interfaces

Figs. 7 and 8, taken from two different areas of the same sample, show high-resolution images of the carbon–silicon carbide interface. On the side of the interfaces labeled ‘A’ in Fig. 7 and ‘B’ in Fig. 8, the interface appears quite well-defined, and it is seen that the highly aligned basal planes of the pyrocarbon appear to be almost parallel to the interface. Such preferred orientation of the basal planes of graphite (and other compounds possessing similar turbostratic layered structures such as boron nitride) relative to substrate surfaces during CVI have been observed by other researchers [12,21,25,27]. The somewhat parallel orientation of the basal planes relative to the interface is believed to be maintained in the vicinity of the interface, but farther away from the interface, the basal planes are expected to be more randomly oriented. On the other side of the C–SiC interfaces (labeled ‘B’ in Fig. 7 and ‘A’ in Fig. 8), the graphite basal planes consistently did not exhibit high alignment, and the interface did not appear to be very defined.

In this work, the carbon layer at the well-defined interfaces was deposited prior to the deposition of the intervening SiC layer, and growth of the carbon layer

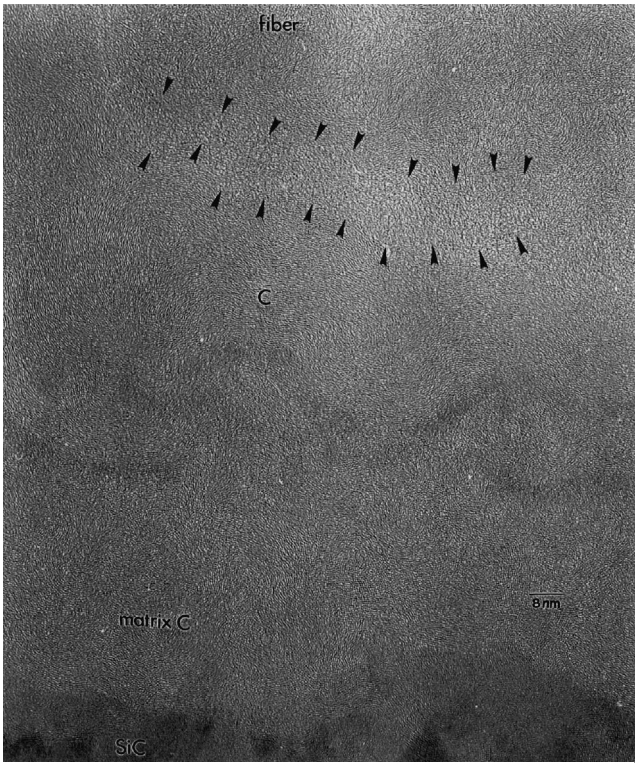

Fig. 4. A high-magnification TEM image of carbon–carbon interfacial zones showing graphitic layers of fiber (F), fiber coating (C), and matrix layers of C and SiC.

terminated at these defined interfaces (labelled ‘A’ in Fig. 7 and ‘B’ in Fig. 8). Thus, the graphite basal planes for the carbon layer seem to become increasingly aligned as growth proceeds. The intervening SiC layer then grows on top of the highly oriented graphite layers at the well-defined interface. However, at the interface labeled ‘B’ in

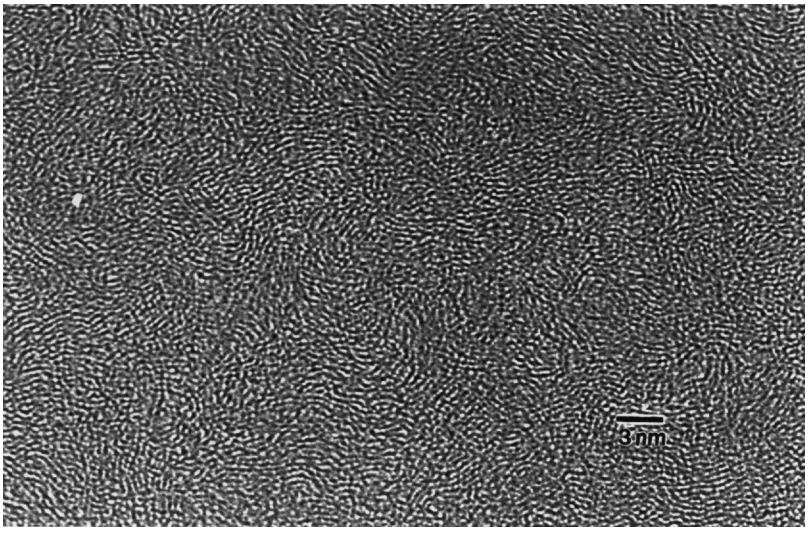

Fig. 5. A high-magnification TEM cross-sectional image of the carbon fiber.

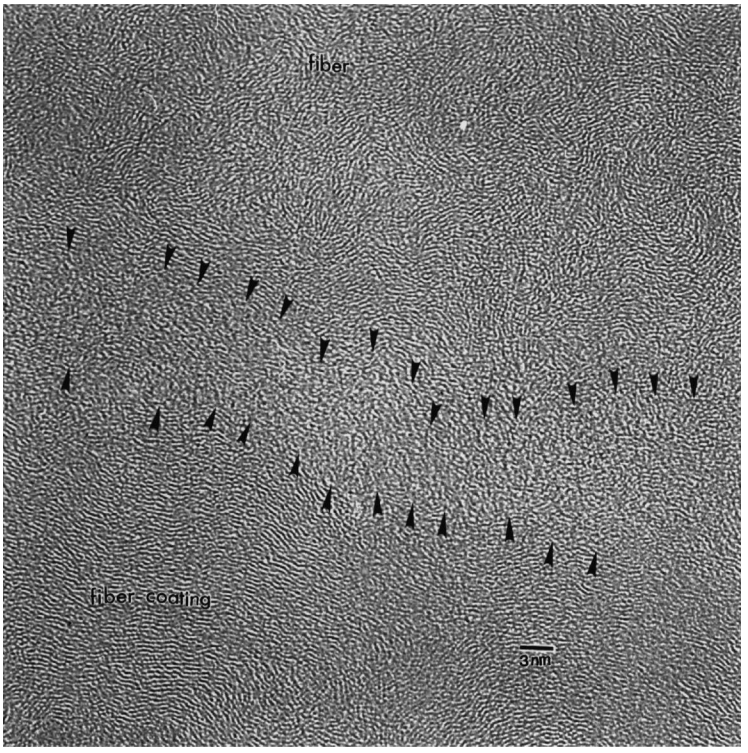

Fig. 6. A high-magnification TEM image of fiber/coating interface depicting thin, transitional layer at the interface.

Fig. 7 and 'A' in Fig. 8, the graphite layers are forced to grow around the shape and morphology of the pre-existing SiC layer. It is likely that this orientation of the graphite basal planes relative to the well-defined interfaces is preferentially assumed because it may be particularly conducive to the nucleation and growth of vapor-phase deposited SiC.

The model of SiC crystal growth presented above is

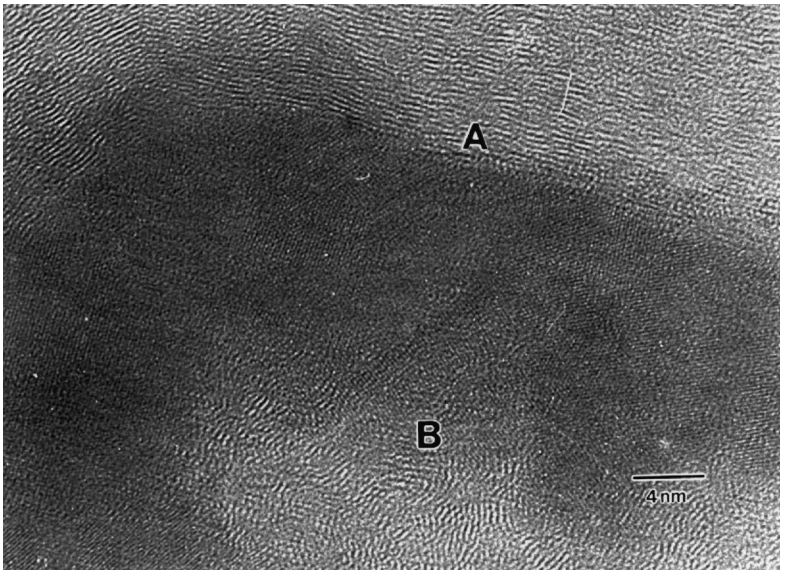

Fig. 7. A high-magnification TEM image of C–SiC interface.

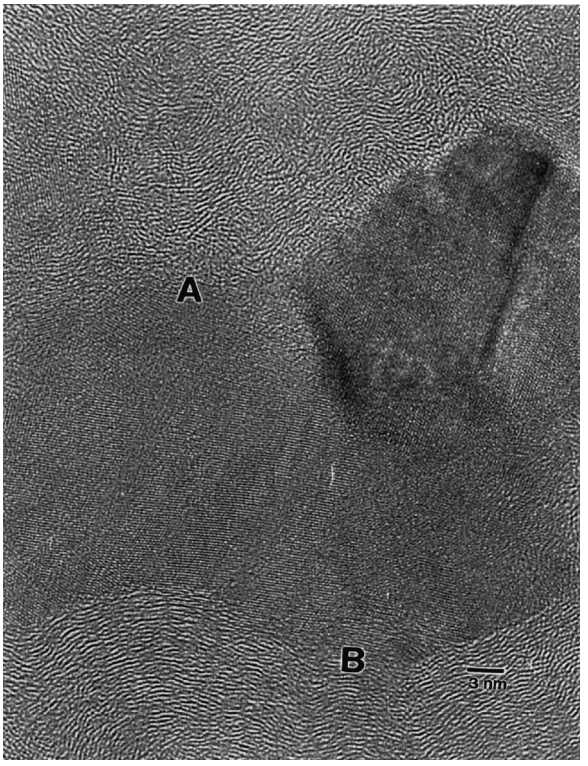

Fig. 8. A high-magnification TEM image of C–SiC interface.

consistent with the morphology of the matrix layers seen in Fig. 3a and b. The side of the C–SiC interface where growth initiates is seen to be smoother at that magnification in comparison to the somewhat jagged outline of the other side of the interface. In fact, the proposed model of SiC growth is in agreement with several published works on the nature of SiC nucleation and growth during vapor-phase deposition. It is well recognized [28–31] that during the vapor-phase deposition of SiC, nucleation and growth commence as a uniform crystalline layer, which subsequently progresses to a competitive growth stage that produces larger columnar grains. This mechanism of nucleation and growth explains why the side of the interface where SiC nucleation initiates is smoother, whereas the side where growth terminates is more irregular. It has also been suggested that for a turbostratic layered structure such as boron nitride (on carbon fibers), such an interfacial orientation is necessary to minimize residual thermal stresses [12] at the interface.

It is well recognized that such an interfacial orientation should be very favorable for fracture toughness improvements of the material [12,26,27]. Although delamination could possibly occur for any orientation of the graphite planes, it is expected that, in this orientation, load transfer would be more easily facilitated and delamination at the interface could easily occur due to the low interfacial shear strength arising from the weak π-bonding between the basal planes of the carbon. Of course, whether delamination will occur preferentially at the SiC–C interface or rather within the carbon layer depends on the strength of the matrix interfacial bonding relative to the *c*-axis bond between the basal planes of the pyrocarbon and their orientation.

4. Conclusions

In this work, the microstructure of interfaces in laminated matrix composites of alternate SiC and carbon layers with carbon-fiber reinforcements has been characterized in detail using TEM. The carbon–carbon interfaces were generally not very clearly defined. However, the interfaces between the fiber and its coating and between the coating and the matrix carbon exhibited important and interesting microstructural features. The C–SiC interfaces within the matrix did exhibit interesting features. One side of the C–SiC interface consistently appeared to be relatively well-defined, whereas the other side of the interface appeared to be more diffuse and less clearly defined. At the well defined C–SiC interfaces, the graphite basal planes were oriented almost parallel to the interface. An understanding of the nucleation and growth of SiC and carbon during CVI is paramount to achieving control of microstructural development during processing in order to obtain composites that will exhibit the desired mechanical properties.

Acknowledgements

This work was supported by the National Science Foundation (NSF Award # DMR-96-32823). Also, one of the authors, K.A. Appiah, is supported by The David and Lucile Packard Foundation.

References

[1] Gadkaree KP, Chyung Y. Am Ceram Soc Bull 1986;65(2):370–6.
[2] Tiegs TN, Becher PF. Mater Sci Res 1986;20:639–47.
[3] Samanta SC, Musikant S. Ceram Eng Sci Proc 1985;6:663–72.
[4] Lundberg R, Kahlman L, Pompe R, Carlsson R, Warren R. Am Ceram Soc Bull 1987;66(2):330–3.
[5] Homeny J, Vaughn WL. MRS Bull 1987;12(7):66–71.
[6] Singh M, Dickerson RM, Olmstead FA, Eldridge JI. J Mater Res 1997;12(3):706–13.
[7] Gopal M. In: Proceedings of the Annual Meeting of Microscopy and Microanalysis, Cleveland OH, August, vol. 3, 1997, Supplement 2.
[8] Brennan JJ. Mater Sci Eng 1990;A126:203–23.
[9] Brennan JJ, McCarthy G. Mater Sci Eng 1993;A162:53–72.

[10] Kerans RJ, Hay RS, Pagano NJ, Parthasarathy TA. Am Ceram Soc Bull 1989;68(2):429–50.
[11] Lewis MH, Murthy VSR. J Comp Sci Technol 1991;42:221–49.
[12] Cofer CG, Economy J, Xu Y, Zangvil A, Lara-Curzio E, Ferber MK, More KL. J Comp Sci Technol 1996;56:967–75.
[13] Kerans RJ, Parthasarathy TA, Jero PD, Chatterjee A, Pagano NJ. Br Ceram Trans 1993;92:181–96.
[14] Mackin TJ, Warren PD, Evans AG. Acta Metall Mater 1992;40:1251–7.
[15] Lackey WJ, Vaidyaraman S, More KL. J Am Ceram Soc 1997;80(1):113–6.
[16] Droillard C, Lamon J, Bourrat X. In: Proceedings of the Fall Meeting of the Materials Research Society, Boston, MA, November, vol. 325, 1994.
[17] Droillard C. Ph.D. Thesis, France: University of Bordeaux, 1993.
[18] Shi R, Hu G, Li H, Kang M. Interfacial microstructures of intrabundle in as-received carbon/carbon composites prepared by CVI. Carbon 1998;36(9):1331–5.
[19] Weizhou P, Tianyou P, Hanmin Z, Qiao Y. In: Proceedings of the Second International Conference on Composite Interfaces (ICCI-II), Cleveland, OH, June, 1988.
[20] Vaidyaraman S. Ph.D. Thesis, Atlanta, GA: Georgia Institute of Technology, 1995.
[21] Savage G. Carbon–carbon composites, New York: Chapman and Hall, 1993.
[22] Lieberman ML, Pierson HO. Carbon 1974;12:233.
[23] Pierson HO, Lieberman ML. Carbon 1975;13:159.
[24] Lewis JS, Lackey WJ, Vaidyaraman S. Carbon 1997;35(1):103–12.
[25] Becker A, Huttinger KJ. Carbon 1998;36(3):201–11.
[26] Dugne O, Prouhet S, Guette A, Naslain R, Fourmeaux R, Khin Y, Sevely J, Rocher JP, Cotteret J. J Mater Sci 1993;28:3409–22.
[27] Grathwohl G, Hahnel A, Meier B, Pippel E, Richter G, Woltersdorf J. J Eur Ceram Soc 1992;10:1–12.
[28] Buchanan FJ, Little JA. Surf Coat Technol 1997;46:227–32.
[29] Shinozaki SS, Sato H. J Am Ceram Soc 1978;61(9–10):425–9.
[30] Pickering MA, Taylor RL, Goela JS, Desai HD. In: Proceedings of the Fall Meeting of the Materials Research Society, Boston MA, November, vol. 250, 1992.
[31] Cheng DJ, Shyy WJ, Kuo DH, Hon MH. J Electrochem Soc 1987;134(12):3145–9.